Langmuir

Article

pubs.acs.org/Langmuir

Simultaneous Measurement of Mechanical and Surface Properties in Thermoresponsive, Anchored Hydrogel Films

Kathryn A. Melzak,[†,‡] Anca Mateescu,[§] José L. Toca-Herrera,[*,†,‡] and Ulrich Jonas[*,§,∥]

[†]Laboratory of Biophysics, Department of Nanobiotechnology, University of Natural Resources and Life Sciences Vienna (BOKU), Muthgasse 11/|| A-1190 Vienna, Austria

[‡]CIC biomaGUNE, Paseo Miramón 182, 20009 San Sebastian, Spain

[§]FORTH, IESL, Bio-Organic Materials Chemistry Laboratory, Nikolaou Plastira 100, Vassilika Vouton, 71110 Heraklion, Crete, Greece

[∥]Macromolecular Chemistry, University of Siegen, Adolf-Reichwein-Strasse 2, 57076 Siegen, Germany

Supporting Information

ABSTRACT: Hydrogel films have been used extensively in the preparation of biosensors and biomedical devices. The characteristics of the aqueous interface of the polymer layer are significant for the biosensor or device function; likewise, the changing mechanical properties of thermoresponsive polymers are an important feature that affects the polymer behavior. Atomic force microscopy was used here to characterize both the surface and the mechanical properties of polymeric hydrogel films prepared from a thermoresponsive terpolymer of *N*-isopropylacrylamide and acrylic acid with benzophenonemethacrylate as a photoreactive cross-linker comonomer. The force−distance curves thus obtained were analyzed to assess both the surface forces and the mechanical response that were associated with the hydrogel. These properties were investigated as a function of temperature, in water and in Tris buffer, for different degrees of polymer cross-linking. For samples in water, the distance over which the surface forces were effective was found to remain constant as the temperature was increased from 26 to 42 °C, even though the mechanical response indicated that the samples had been heated past the lower critical solution temperature, or LCST. The bulk of the polymer becomes less soluble above the LCST, although this does not seem to affect the surface properties. This may be due to the segregation of the acrylic acid-rich polymer segments near the gel surface, which is in agreement with reports for related systems.

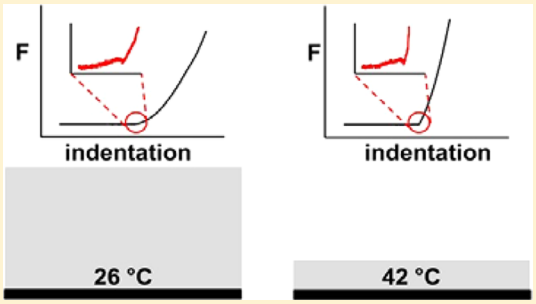

INTRODUCTION

The responsive behavior of surface-attached hydrogel films has attracted interest because of the applications that such layers have in tissue engineering,[1−3] controlled drug delivery,[4,5] optical sensing devices, and actuators.[6−9] Homopolymers based on *N*-isopropylacrylamide (NIPAAm) are well known to respond to changes in temperature and exhibit a lower critical solution temperature, or LCST, of about 32 °C, which is close to body temperature. These polymers precipitate into a compact state at temperatures above the LCST, although at temperatures below the LCST, they retain a high solubility in water; the response to temperature is thus a change in size and an associated change in the mechanical properties as the polymer becomes more compact. Thermoresponsive polymers of NIPAAm have been given properties in addition to their thermal sensitivity by the incorporation of other comonomers.[10] The copolymers thus formed can retain the thermoresponsiveness of the parent PNIPAAm while gaining new features associated with the physical and chemical properties of the second homopolymer. The copolymerization of NIPAAm with ionic monomers has produced polymers that are responsive to both temperature and pH,[11−13] and temperature-sensitive biodegradable polymers have been prepared by the copolymerization of NIPAAm with appropriate monomers.[14,15]

Copolymers, in addition to their ability to incorporate the properties of two or more components, also have the potential to form structures associated with the phase separation of immiscible blocks.[16,17] One related example of such a phase-separated structure is the macroporous architecture of bulk hydrogels that are formed from PNIPAAm and poly(ethylene glycol) (PEG).[17] The separation of the PEG in this case leads to the formation of hydrophilic pores that increase the response rate of the polymer to external stimuli. The incorporation of charged species in PNIPAAm copolymers has also been suggested as a means of producing hydrophilic channels within the gel.[18] Hydrogels based on 2-hydroxyethyl methacrylate and 2-ethylhexyl acrylate have shown a segregation of the

Received: May 14, 2012
Revised: August 6, 2012
Published: August 6, 2012

components in microdomains, with the 2-hydroxyethyl methacrylate segments being the continuous phase.[19] In general, most block copolymer systems that incorporate a charged species contain water-soluble blocks with the ionic component, and the hydrophobic, neutral block forms the network junctions.[20−23] Recently, however, a new strategy based on the phase-separation of ion-rich regions from the aqueous environment driven by complex coacervate formation has been reported,[23] where the ionic end blocks in two oppositely charged ABA PEG block copolymers aggregate from solution to form a hydrogel structure.

If block copolymers are formed into thin films, then the separation into microdomains can lead to the formation of numerous different film morphologies. The structural arrangements produced will be a function of the block and domain sizes, the film thickness, and the relative affinities of the different domains for the substrate and the solvent.[16,24,25]

The hydrogel films described here have thicknesses on the order of micrometers and are therefore expected to be much thicker than the domain size associated with any potential phase separation. One example of ordering that has been observed in this sort of thick film is the formation of lamellar structures in films of poly(styrene-*co*-methyl methacrylate),[25] where the formation of lamellar structures oriented in the plane of the substrate was found to be dependent on interactions with the substrate and the solvent. Films formed without lamellar structures were found to be able to develop such an arrangement after exposure to solvent at temperatures above the glass-transition temperature for the polymer.[24]

Another structural feature that has been observed on the surface of PNIPAAm gels is the formation of a dense skin above the LCST.[18] The polymer on the outer surface of PNIPAAm blocks[18] or at the periphery of small PNIPAAm globules[26] has been shown to form a temperature-induced compacted layer that can entrap water and various solute molecules within the gel. It has been suggested that the formation of such a layer can contribute to the stability of globules of PNIPAAm copolymers by acting to prevent interparticle aggregation through a viscoelastic stabilizing effect in which the polymer chain relaxation time becomes longer than the collision time, thus preventing adhesion during collisions.[18,27] In addition, hydrophilic segments of PNIPAAm copolymers may be located at the aqueous periphery,[28] thus providing an alternative mechanism for stabilizing polymer globules by their effects on interparticle interactions.

The PNIPAAm terpolymer samples characterized within this work are thin surface-supported films, one of the most convenient formats for sensor applications. The ionic groups introduced into the film prevented the formation of an outer skin above the LCST; optical studies have shown that the collapse originates instead from the center of the film.[29] The measured optical gradient profiles showed that the density of these gels decreases steadily over a transition regime adjacent to the aqueous phase. The thickness of the transition regime varies with temperature and is relatively large (up to 4 μm) just below the LCST while being quite small (0.5 μm) just above the LCST.[29] Differences between the behavior of films and bulk gel may be associated with the swelling restrictions imposed by the anchoring of the film to the substrate, which has the effect of restricting the film expansion, preventing lateral swelling, and permitting expansion only in the direction normal to the substrate surface.[30]

At the LCST, soluble PNIPAAm becomes insoluble in water and cross-linked PNIPAAm blocks or films collapse, as does end-tethered PNIPAAm in brushes;[31] in general, the extent of interaction with water changes, leading to the possibility that the surface hydrophilicity changes. For the work presented here, an atomic force microscope was used to investigate the mechanical and thermoresponsive properties of the PNIPAAm-based hydrogel films as well as the surface forces. Force−distance curves can be divided into noncontact and contact regions, representing the response of the cantilever before and after the tip makes contact with the sample. The contact region of the force−distance curves provides information about the sample deformability, and the noncontact region provides information about surface properties such as surface charge. For the PNIPAAm terpolymer films investigated here, the contact region was analyzed to confirm the temperature-induced collapse that occurs as the films are heated to above the LCST. Features near the estimated contact points were analyzed and provided evidence that the surface forces remained constant during this phase transition. The model suggested here to explain these results is based on the segregation of the more polar polymer sequences on the surface of the hydrogel films, as will be described below.

EXPERIMENTAL PART

Materials. All chemicals were used as received unless noted otherwise. Ultrapure water was obtained by ultrafiltration through a Millipore filter system.

Polymer Synthesis. A terpolymer based on NIPAAm (94% monomer concentration), acrylic acid (AA, 5% m.c.), and 4-benzophenonemethacrylate (BPMA, 1% m.c.) was prepared by free radical polymerization in dioxane with 2,2′-azobis(2-methylpropionitrile) (AIBN) as an initiator. Details of the synthesis and characterization of the terpolymer are described elsewhere.[32] A molecular weight (M_w) of 206 kg mol^{-1} and a polydispersity index (M_w/M_n) of 2.0 were measured by gel permeation chromatography, and the polymer composition resembled the monomer feed composition as revealed by the ^{1}H NMR spectrum.

Polymer Films. Glass substrates pretreated with a Hellmanex solution were subsequently silanized with an ethanolic solution of 4-(triethoxysilyl propyloxy)benzophenone (1 mM) overnight. A 10 wt % solution of the polymer in ethanol was spin-coated at 4000 rpm for 60 s on the silane-modified glass slides. The polymer films were then dried in vacuum for 3 h at 50 °C before being cross-linked by UV irradiation with a wavelength of 365 nm at an irradiation dose of 0.1 J cm^{-2}min^{-1}. Both cross-linking and surface attachment were simultaneously induced by UV irradiation, and the degree of cross-linking was controlled by the irradiation time. The polymer films were stored dry, cool, and in the dark until use.

Atomic Force Spectroscopy Measurements. All measurements were made with a JPK Nanowizard 2 AFM (JPK Instruments, Germany) using uncoated MLCT chips with cantilevers having a nominal spring constant of 0.1 N/m and pyramidal silicon nitride tips with a nominal tip radius of 20 nm (Veeco Instruments, USA). The unmodified tips were used because they were small on the scale of the surface buckling associated with the swelling restrictions imposed by film anchoring (Figure A1, Supporting Information). Spring constants were determined precisely at the start of each experiment. This was done at one temperature only; the value obtained at room temperature was then used for all subsequent calculations. An initial calibration showed that the sensitivities and spring constants did not vary significantly with temperature. Chips were cleaned with argon plasma or by oxidation with basic hydrogen peroxide (50 mL of water was added to 10 mL of ammonium hydroxide and heated to 70 °C; 10 mL of 30% H_2O_2 was added and the chips were immersed in the solution for about 10 s). The samples were heated to 50 °C and then cooled to 25 °C before the start of the measurements in order to dissolve non-

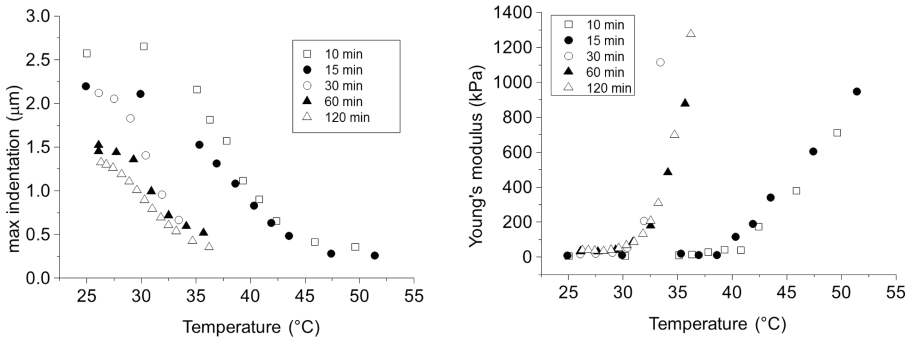

Figure 1. Collapse of the P(NIPAAm-*co*-AA-*co*-BPMA) terpolymer films as a function of temperature for different cross-linking times; the collapse is indicated by the maximum indentation at 40 nN (left) and by the values of Young's modulus (right).

cross-linked polymer fractions. The force curves were acquired at different temperatures while heating the sample using the JPK BioCell heater, which heats the solution immediately above the sample surface; samples were left to equilibrate for at least 10 min after each temperature increment before measurements were made. The initial position of the cantilever was not adjusted between measurements unless necessary because of the change in the height of the polymer. Additional force−distance curves were acquired as the sample was cooled in order to confirm the reversibility of the temperature-induced collapse. The force−distance curves were acquired at tip approach and retraction rates of 1 μm/s and maximum loads of 40 nN, unless otherwise specified.

Analysis of the Force−Distance Curves. The graphs of applied load (cantilever deflection) as a function of tip−sample separation are referred to here as force−distance curves. Data obtained during measurements were converted to force−distance curves using the values calculated for the cantilever spring constants in each experiment and subtracting the value of the cantilever deflection from the changes in the position of the piezoelectrically driven stage. The curves were analyzed, again using the JPK instrument software, to determine Young's modulus, the maximum indentation, the observed contact point, and the contact point according to Young's modulus fitting. Young's modulus was determined by fitting data with the Hertz model modified for square-pyramidal tips in which the force is given by $F = 0.7453(E/(1 - \nu^2))\delta^2 \tan \alpha$, where F is the force, E is Young's modulus, ν is Poisson's ratio, which is assumed to be 0.5, δ is the indentation, and α is the face angle of the pyramid.[33]

The tips did not reach the incompressible substrate at any point during the measurements, which means that the measured indentation will be less than the thickness of the polymer (Figure A2, Supporting Information). The indentation will be a function of both the intrinsic properties of the polymer (polymer softness) and experimental conditions such as the maximum applied load. The measured indentation can be used to determine the relative changes in polymer properties within one set of experiments but does not give an absolute value suitable for comparison with data from other sources.

Values obtained for Young's modulus from AFM force−distance curves are considered to be reasonable estimates if the sample exhibits elastic behavior over the indentation range investigated and if the maximum indentation is less than 10% of the sample thickness.[34]

For the experiments described here, the first condition was met by determining Young's modulus using the indentation range over which the observed data followed the model described above. The elastic behavior of the samples over this range was confirmed by the linear response observed when the force was graphed against the square of the indentation (Figure A3, Supporting Information). The data range used for these calculations was typically between one-third and one-half of the maximum indentation. Using the full data range produced estimates of Young's modulus values that were, for the softer samples (<50 kPa), similar to the values obtained using the smaller data range; for the collapsed layers at higher temperatures, using the full data range produced values that were substantially lower (by a factor of 3 or more; data not shown).

The total film thickness has been measured previously for samples prepared in a way similar to that used here[29] and was found to be about 5.5 μm in water at 22 °C; as will be shown below, the maximum indentations measured for analogous samples and sample conditions were about 2 μm, so that the range used for calculations was between 10 and 20% of the total sample thickness. The values presented here for Young's modulus are therefore only approximations; they provide a measure to determine the collapse of the polymer but are only a rough guide for comparison to stiffness values measured for other samples.

RESULTS AND DISCUSSION

Temperature-Dependent Collapse of the Supported Films as a Function of Cross-Linking Time. Hydrogel samples of PNIPAAm are known to collapse as the temperature is increased above the lower critical solution temperature, or LCST. The PNIPAAm changes at this point from a relatively diffuse gel with a high water content to a more compact form in which much of the water is expelled. For surface-supported films, the temperature at which this collapse occurs is affected by the constraints associated with the swelling of films that have been cross-linked when in the dry state.[35] The film thickness and the location within the hydrogel film with respect to the aqueous interface affects the transition temperature,[35] as does the degree of cross-linking.[29,35] This means that the collapse is dependent on the conditions associated with the film preparation, and that the transition temperature must be determined experimentally for new film preparation conditions.

The feature that has been used in these experiments to characterize the transition temperature is the change in the mechanical properties associated with the formation of the more compact state of the polymer rather than the change in layer thickness that occurs during the collapse. The mechanical properties were assessed by determining the indentation at a fixed maximum applied pressure and by determining the values for Young's modulus, as shown in Figure 1. Indentation values proved to be more helpful for determining the transition temperature; as may be seen in Figure 1, these curves had an s shape, where the transition temperatures can be associated with the inflection points. Values obtained for Young's modulus did not reach a constant value as the temperature was increased; the Young's modulus results in Figure 1 show that the different samples collapse at different temperatures but there is no simple way to identify values for the transition temperature. The indentation was therefore used in subsequent experiments as a measure of the film properties. The values observed for maximum indentation at 40 nN are in good agreement with the values that can be calculated from the Young's modulus using

dx.doi.org/10.1021/la3019666 | *Langmuir* 2012, 28, 12871−12878

the modified Hertz model described above, as illustrated in Figure A4 in the Supporting Information.

Figure 1 shows that films with cross-linking times of 30 min or more collapse at a temperature similar to the 32 °C value given for the LCST of bulk PNIPAAm.[36] Lower cross-linking times, however, lead to the higher transition temperatures that have been associated with the stresses in surface-supported films.[35] This increase in the transition temperature was about 10 K for the 10 and 15 min cross-linked samples and more than 10 K for a 5 min cross-linked sample (Figure A5, Supporting Information). Subsequent studies were done with polymer films that had been cross-linked for times between 30 and 120 min in order to avoid the thin film effects.

One additional advantage of films with longer cross-linking times is that they show greater long-term stability; films prepared with very short cross-linking times detached from the surface after some hours in water. It may be noted that the mechanical properties of the polymers change over time during storage in water, as shown in Figure A6 of the Supporting Information. To circumvent this problem, samples were stored overnight prior to the start of the measurements for all experiments other than those used for Figure 1, where samples were measured on the first day in water in order to be able to look at a greater range of cross-linking times.

Effect of Buffer on the Film Properties. The addition of buffer at pH 7 increased the temperature at which the films collapsed, as shown in Figure 2. It is, however, clear that the polymer films retain their LCST behavior for cross-linking times of between 30 and 120 min. The maximum indentation is also reduced in the presence of buffer, as indicated in Figures 3 and 4. The buffer will affect both the degree of ionization of the acrylic acid groups and the Debye screening length, as has been described in a theoretical model for a weak polyacid network under good-solvent conditions.[37] It is the former effect that is apparent here: greater ionization of the PAA block of the PAA-PNIPAAm copolymer is known to increase the temperature at which the copolymers collapse.[11,38] This effect is due to the increased solubility of the ionized PAA and is known to be much more prominent for bulk gels than for dispersed microparticles.[38] The Tris buffer at pH 7 consists mostly of tris(hydroxymethyl)aminomethane hydrochloride, which will dissociate into the Tris cation and the chloride anion. To a first approximation, the solution may therefore be considered to be a 0.001 M fully dissociated solution, which would have a Debye length of about 10 nm.

Features near the Contact Point on the Force–Distance Curves. When the force–distance curves were measured in water, the films showed a bump near the contact point, as illustrated in Figure 3. This feature disappeared in Tris buffer, as shown in Figure 4.

One of the challenges with deformable samples is to determine the position of the surface. There is no clear demarcation between the noncontact and contact regions of the force–distance curves; in addition, soft materials such as the films investigated here can show significant deformation before contact.[39] The approach taken here has been to equate the surface position with the contact point that is estimated from the Hertz model fitting, as indicated in Figures 3 and 4. The force–distance curves were analyzed as described in the Experimental Part and in Figure A3 of the Supporting Information in order to obtain values for both Young's modulus and the contact point. As is shown in Figure 3, the contact point that may be obtained from the Hertz model fit

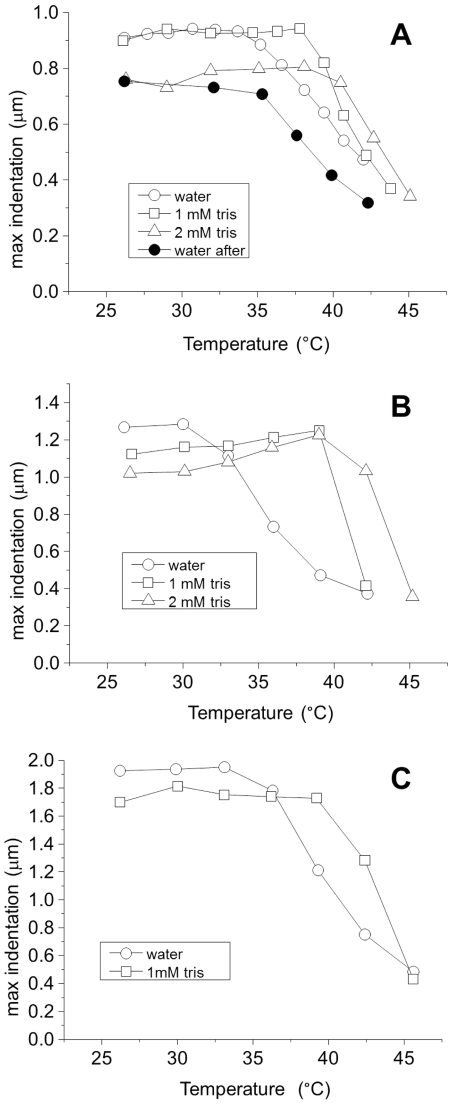

Figure 2. Temperature-induced collapse of the films at different Tris concentrations for films prepared with (A) 120, (B) 60, and (C) 30 min cross-linking times. Measurements for the 120 min sample were made in the sequence water–1 mM Tris–2 mM Tris–water after. Although the maximum indentation decreases in the second measurement sequence in water, the collapse temperature remains the same.

does not correspond to the point at which the force–distance curves deviate from the baseline. The difference between the value obtained from the model and the observed deviation from the baseline was then calculated for force–distance curves measured at different temperatures on films prepared at different cross-linking times; these values are shown in Figure 5.

Figure 5 is therefore presented as an indicator of the difference between the observed data and the Hertz model fitting, which is attributed here to the noncontact interactions. More detailed characterization of the noncontact interactions is affected by the fact that this region in the force–distance curves is not differentiated from the contact region, as can be seen in Figure 3. The analysis presented here is therefore limited to showing that the noncontact interactions remain constant as a function of temperature for polymer films with different cross-linking times; this will be discussed briefly below, followed by a discussion of the implied surface structural arrangements.

dx.doi.org/10.1021/la3019666 | Langmuir 2012, 28, 12871–12878

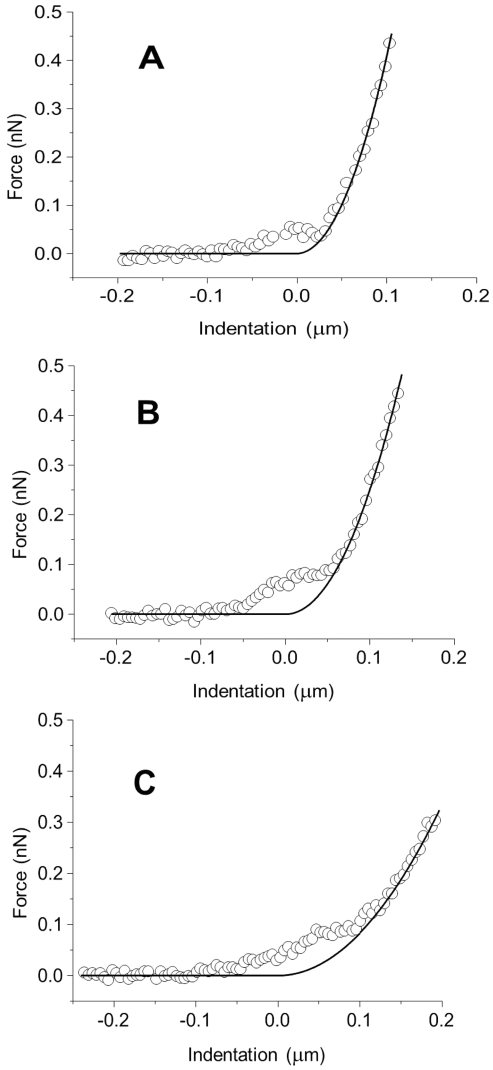

Figure 3. Force−distance curves near the contact point for the P(NIPAAm-*co*-AA-*co*-BPMA) terpolymers in water at 26 °C for films prepared with cross-linking times of (A) 120, (B) 60, and (C) 30 min. Data points (only every 10th acquired point shown) are presented as open circles. The solid lines are composites of one section of baseline, and a second section, from the contact point onward, generated from the Hertz model as modified for pyramidal tips, with values of Young's modulus equal to (A) 56.1, (B) 35.9, and (C) 11.9 kPa. The indentation is calculated relative to the location of the surface as extrapolated from the Hertz model fitting.

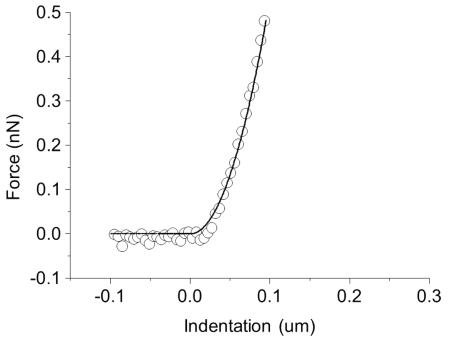

Figure 4. Tip−sample contact region of the force−distance curve for the 120 min cross-linked P(NIPAAm-*co*-AA-*co*-BPMA) film in 1 mM Tris buffer at 26 °C. Data points (only every 10th acquired point shown) are presented as open circles. The solid line indicates the fit to the model, with a Young's modulus of 76.8 kPa being substantially larger than the corresponding value of 56.1 kPa in pure water (Figure 3A).

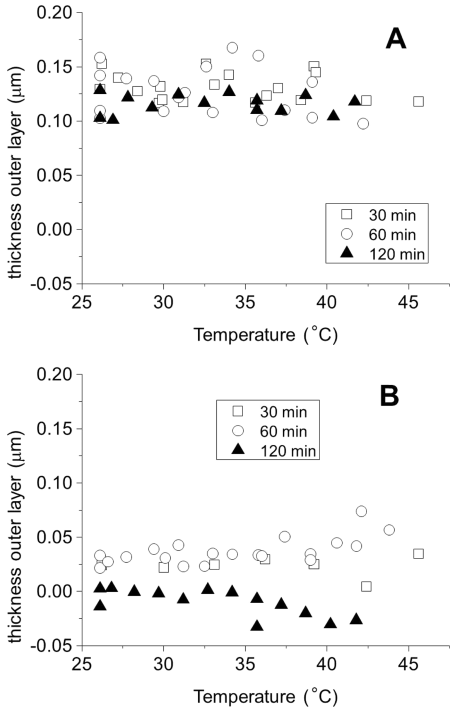

Figure 5. Difference between the observed deviation from the baseline and the value of the contact point as estimated from the theoretical fitting (Figure 3) for films in (A) water and in (B) 1 mM Tris, with cross-linking times as shown in the figure legends. Values shown here include measurements made on different samples.

Features similar to the bump in Figure 3 can be produced by a combination of noncontact forces that act over different length ranges.[39,40] If the tip of the AFM cantilever has the same charge as the sample surface, then electrostatic interactions can cause an initial repulsion. As the tip approaches sufficiently closely, stronger but shorter-ranged forces, such as van der Waals forces, can overcome the resistance of the cantilever and the electrostatic repulsion so that the tip snaps into contact with the surface. For the sample and tip considered here, electrostatic interactions in water will be repulsive because the tip will be negatively charged due to the silica layer that coats the silicon nitride surface, whereas the acrylic acid groups of the polymer film will be negative under the slightly acidic conditions (pH 5.6) resulting from the dissolution of CO_2 in air but will be only partially ionized.[41] The attractive forces seen here could be due to van der Waals interactions. An alternative source of attraction would be bridging interactions between the AFM tip and the dangling ends of polymers protruding into solution. When PNIPAAm copolymers are produced as brushes, such bridging interactions have been postulated as a source of long-range attraction.[42] This could explain the fact that the attractive forces here seem to occur over a range longer than that typically associated with van der Waals interactions.

The bump in Figure 3A becomes much less prominent on films that are more deformable, such as Figure 3C. However, this may be merely a result of adding different curve shapes: when the curves for the Hertz model fits are subtracted from the data curves in Figure 3, the resulting difference is the same for all three samples (Figure A7 in the Supporting

dx.doi.org/10.1021/la3019666 | *Langmuir* 2012, 28, 12871−12878

Information). The noncontact interactions therefore seem to be unaffected by the degree of cross-linking in the polymer film. The apparent snap-to-contact distance here (describing the region of negative slope in Figure 3a) is a function of the softness of the material under investigation.

For electrostatic repulsion, the force decays exponentially with distance. Because the repulsion will be dependent on the shape of the AFM tip, the measurements for Figure 5 were acquired with one tip over the full range of temperatures and then repeated with a second tip from the same batch. The characteristic decay lengths were estimated by replotting the force−distance curves as the force versus tip−sample separation and then fitting a 150 nm segment of the curve to an exponential decay function (cf. Figure A7, Supporting Information). A decay length of 53 nm was estimated for the 120 min cross-linked sample on the basis of an average of measurements at all temperatures; this corresponds to the Debye length associated with a 1:1 electrolyte concentration of 0.04 mM. This would be higher than the 0.0025 mM expected for a saturated solution of CO_2. One possible explanation for the discrepancy is that soluble material could be released from the polymer film, while a second possibility is that the region of the force−distance curve that was analyzed is affected by both the electrostatic repulsion and the sample deformability. This second hypothesis certainly seems to apply to the decay length values estimated for measurements on the films with shorter cross-linking times, which showed increasing values (to 70 and 90 nm for the 60 and 30 min cross-linking times).

We are proposing here that the values displayed in Figure 5 indicate the extent of the electrostatic repulsion. Although we do not measure the absolute value of the surface charge density, we can look at relative changes: we know that the tip shape and the solution properties remain constant, and we can therefore say that the surface charge density also appears to remain constant. The surface charge therefore appears to remain constant as the films are heated to above the temperature at which they collapse, and as the cross-linking time of the films changes.

The addition of Tris should increase the degree of ionization on the acrylic acid groups, as discussed above; however, as is also mentioned, 1 mM Tris will decrease the Debye length of the solution.

There is no evidence of electrostatic repulsion in these force−distance curves, but this may be because the expected shape of the curve (an exponential decay with a decay length of 10 nm) is not readily distinguishable from the contact region of the force−distance curve (which can be approximated near the contact point as an exponential decay with a decay length of 15 nm).

Possible Causes and Implications of Constant Surface Charge. As mentioned in the Introduction, it is possible for block copolymers to undergo phase separation, with the formation of separate domains.[16,24,25] Copolymers of PNIPAAm and PAA have been prepared as microparticulate gels; in these cases, PAA has been shown to be on the outside of the particles.[41,43] These copolymer particulates have been observed to have a densely cross-linked core, with a soft outer shell that can have a thickness of 100 nm or more.[43] It is also possible to assemble aggregates of PNIPAAm-PAA copolymers in which PAA is on the interior because of the interaction with a positively charged micellar core.[44] In this case, the exterior layer remains thermoresponsive and collapses with increasing temperature.

The P(NIPAAm-*co*-AA-*co*-BPMA) copolymer used to prepare the hydrogel films described in this article is synthesized by the free radical copolymerization of NIPAAm, acrylic acid (AA), and benzophenonemethacrylate (BPMA). An analysis of this copolymer has shown that the mole ratio of monomer present in the product is the same as in the monomer feed for the reaction.[45] However, this analysis does not provide information regarding the monomer distribution, a factor that affects copolymer properties and that can be predicted by a consideration of the reactivities of the different monomers.[46] Analysis of the copolymerization parameters for this type of copolymerization among NIPAAm, AA, and BPMA indicates a preference for the incorporation of AA or BPMA into the NIPAAm-terminated chain, whereas AA and BPMA units at the chain end show a slight preference for homopolymerization.[47] It would therefore be possible to have compositional heterogeneity along an individual polymer chain with acrylic acid-rich domains.

Contact angle measurements that have been made previously on PNIPAAm have shown that the polymer is capable of reorienting, depending on the medium in contact with the polymer. When the polymer surface was exposed to air, the advancing contact angles of water droplets indicated a relatively hydrophobic surface, with hydrophobicity that increased at temperatures above the LCST; the receding contact angles, however, indicated a relatively hydrophilc surface, a feature that was retained even above the LCST.[48] In addition, contact angle measurements with air bubbles on PNIPAAm in an aqueous environment indicate that the polymer remains hydrophilic, in contrast to the hydrophobicity indicated by the advancing water droplets in air.[49] The properties of the surface layer are relevant to sensor and tissue engineering applications because it is the aqueous face of the film that will make contact with the analyte. The evidence presented here suggests that the aqueous interface of the terpolymer film may not be thermoresponsive, even if the bulk of the film is.

We therefore propose that the acrylic acid-rich segments and dangling chain ends of the terpolymer network orient toward the aqueous interface and that this orientation is retained as the polymer films are heated to above the LCST, when water is expelled from the bulk of the film. This would be in agreement with the contact angle results on PNIPAAm and with other studies on PNIPAAm-PAA copolymers discussed above.

Features similar to the bumps in Figure 3 have been seen previously in association with the disruption of thin soft layers.[50] Although we are proposing that a thin layer is formed at the aqueous interface, we are also suggesting that it is the surface forces associated with such a layer rather than mechanical disruption that lead to the characteristics of Figure 3. The uniformity of the thickness measurements, while expected for an effect due to surface forces, would not be expected for the thicknesses of features on a molecular scale. The 130 nm value of the measured thickness of the outer layer is comparable to the expected polymer contour length of about 200 nm; if our results were solely due to the mechanical disruption of a thin film, then we would expect a variation in the results reflecting the polydispersity (of 2) for the whole molecule, the distribution of sizes of the acrylic acid-rich domains, and the probability of interacting with a single molecule during any one AFM measurement. The attribution of the features in Figure 3 to surface forces is plausible, and the attribution to the mechanical disruption of a thin layer therefore seems unlikely. However, the essential conclusion of

this work is supported equally by both explanations. We are suggesting that the surface characteristics of the polymer films remain constant as the films are heated past the LCST; we have stated that this is indicated by a constant charge density, but it would be supported equally by the constant presence of a thin collapsible film.

The force−distance curves are presented here as a way to investigate the outer surface of supported films prepared from block copolymers while simultaneously confirming the temperature-induced collapse of the film.

■ ASSOCIATED CONTENT

Supporting Information

Images acquired with a CCD camera from Imaging Source indicating that the sample surface buckled during the heating of the polymer films. Force−distance curves. Force versus indentation squared plots. Comparison of measured and calculated values for indentation at 40 nN. Maximum indentation as a function of temperature for PNIPAAM-poly(acrylic acid) copolymer films with different cross-linking times. Effect of storage time in water. Difference between the force−distance curves acquired in water and the Hertz model fit. This material is available free of charge via the Internet at http://pubs.acs.org.

■ AUTHOR INFORMATION

Notes

The authors declare no competing financial interest.

■ ACKNOWLEDGMENTS

This work was partially supported by the Etortek Program of the Regional Basque Government. This work was partially supported by the European Commission through the ESMI - European Soft Matter Infrastructure project (grand agreement number 262348).

■ REFERENCES

(1) Okano, T.; Yamada, N.; Sakai, H.; Sakurai, Y. A novel recovery system for cultured cells using plasma-treated polystyrene dishes grafted with poly(*N*-isopropylacrylamide). *J. Biomed. Mater. Res.* **1993**, *27*, 1243−1251.

(2) Kushida, A.; Yamato, M.; Konno, C.; Kikuchi, A.; Sakurai, Y.; Okano, T. Decrease in culture temperature releases monolayer endothelial cell sheets together with deposited fibronectin matrix from temperature-responsive culture surfaces. *J. Biomed. Mater. Res.* **1999**, *45*, 355−362.

(3) Tsuda, Y.; Kikuchi, A.; Yamato, M.; Chen, G. P.; Okano, T. Heterotypic cell interactions on a dually patterned surface. *Biochem. Biophys. Res. Commun.* **2006**, *348*, 937−944 8.

(4) Dong, L.-C.; Hoffman, A. S. Synthesis and application of thermally reversible heterogels for drug delivery. *J. Controlled Release* **1990**, *13*, 21−31.

(5) Qiu, Y.; Park, K. Environment-sensitive hydrogels for drug delivery. *Adv. Drug Delivery Rev.* **2001**, *53*, 321−339.

(6) Mateescu, A.; Wang, Y.; Dostalek, J.; Jonas, U. Thin hydrogel films for optical biosensor applications. *Membranes* **2012**, *2*, 40−69.

(7) Wang, Y.; Huang, C.-H.; Jonas, U.; Wei, T.; Dostalek, J.; Knoll, W. Biosensor based on hydrogel optical waveguide spectroscopy. *Biosens. Bioelectron.* **2010**, *25*, 1663−1668.

(8) Bashir, R.; Hilt, J. Z.; Elibol, O.; Gupta, A.; Peppas, N. A. Micromechanical cantilever as an ultrasensitive pH microsensor. *Appl. Phys. Lett.* **2002**, *81*, 3091−3093.

(9) Hilt, J. Z.; Gupta, A. K.; Bashir, R.; Peppas, N. A. Ultrasensitive biomems sensors based on microcantilevers patterned with environmentally responsive hydrogels. *Biomed. Microdev.* **2003**, *5*, 177−184.

(10) Rzaev, Z. M. O.; Dinçer, S.; Pişkin, E. Functional copolymers of *N*-isopropylacrylamide for bioengineering applications. *Prog. Polym. Sci.* **2007**, *32*, 534−595.

(11) Schilli, C. M.; Zhang, M.; Rizzardo, E.; Thang, S. H.; Chong, Y. K. B.; Edwards, K.; Karlsson, G.; Müller, A. H. E. A new double-responsive block copolymer synthesized via RAFT polymerization: poly(*N*-isopropylacrylamide)-*block*-poly(acrylic acid). *Macromolecules* **2004**, *37*, 7861−7866.

(12) Jones, M. S. Effect of pH on the lower critical solution temperatures of random copolymers of *N*-isopropylacrylamide and acrylic acid. *Eur. Polym. J.* **1999**, *35*, 795−801.

(13) Yin, X.; Hoffman, A. S.; Stayton, P. S. Poly(*N*-isopropylacrylamide-*co*-propylacrylic acid) copolymers that respond sharply to temperature and pH. *Biomacromolecules* **2006**, *7*, 1381−1385.

(14) Lee, B. H.; Vernon, B. Copolymers of *N*-isopropylacrylamide, HEMA-lactate and acrylic acid with time-dependent lower critical solution temperature as a bioresorbable carrier. *Polym. Int.* **2005**, *54*, 418−422.

(15) You, Y.; Hong, C.; Wang, W.; Lu, W.; Pan, C. Preparation and characterization of thermally responsive and biodegradable block copolymer comprised of PNIPAAM and PLA by combination of ROP and RAFT methods. *Macromolecules* **2004**, *37*, 9761−9767.

(16) Fasolka, M. J.; Mayes, A. M. Block copolymer thin films: physics and applications. *Annu. Rev. Mater. Res.* **2001**, *31*, 323−355.

(17) Zhang, X.-Z.; Yang, Y.-Y.; Chung, T.-S.; Ma, K.-X. Preparation and characterization of fast response macroporous poly(*N*-isopropylacrylamide) hydrogels. *Langmuir* **2001**, *17*, 6094−6099.

(18) Yu, H.; Grainger, D. W. Thermo-sensitive swelling behavior in crosslinked *N*-isopropylacrylamide networks: cationic, anionic, and ampholytic hydrogels. *J. Appl. Polym. Sci.* **1993**, *49*, 1553−1563.

(19) Vazquez, B; San Roman, J.; Peniche, C.; Cohen, M. E. Polymeric hydrophilic hydrogels with flexible hydrophobic chains. Control of the hydration and interactions with water. *Macromolecules* **1997**, *30*, 8440−8446.

(20) Li, C.; Tang, Y.; Armes, S. P. Synthesis and characterization of biocompatible thermo-responsive gelators based on ABA triblock copolymers. *Biomacromolecules* **2005**, *6*, 994−999.

(21) Xu, C.; Breedveld, V.; Kopecek, J. Reversible hydrogels from self-assembling genetically engineered protein block copolymers. *Biomacromolecules* **2005**, *6*, 1739−1749.

(22) Determan, M. D.; Guo, L.; Thiyagarajan, P.; Mallapragada, S. K. Supramolecular self-assembly of multiblock copolymers in aqueous solution. *Langmuir* **2006**, *22*, 1469−1473.

(23) Hunt, J. N.; Feldman, K. E.; Lynd, N. A.; Deek, J.; Campos, L. M.; Spruell, J. M.; Hernandez, B. M.; Kramer, E. J.; Hawker, C. J. Tunable, high modulus hydrogels driven by ionic coacervation. *Adv. Mater.* **2011**, *23*, 2327−2331.

(24) Chen, Y.; Wang, Z.; Gong, Y.; Huang, H.; He, T. Solvent-induced novel morphologies in diblock copolymer blend thin films. *J. Phys. Chem. B* **2006**, *110*, 1647−1655.

(25) Russell, T. P.; Coulon, G.; Deline, V. R.; Miller, D. C. Characteristics of the surface-induced orientation for symmetric diblock PS/PMMA copolymers. *Macromolecules* **1989**, *22*, 4600−4606.

(26) Junk, M. J. N.; Li, W.; Schlüter, A. D.; Wegner, G.; Spiess, H. W.; Zhang, A.; Hindenberger, D. Formation of a mesoscopic skin barrier in mesoglobules of thermoresponsive polymers. *J. Am. Chem. Soc.* **2011**, *133*, 10832−10838.

(27) Wu, C.; Li, W.; Zhu, X. X. Viscoelastic effect on the formation of mesoglobular phase in dilute solutions. *Macromolecules* **2004**, *37*, 4989−4992.

(28) Vasilevskaya, V. V.; Khalatur, P. G.; Khokhlov, A. R. Conformational polymorphism of amphiphilic polymers in a poor solvent. *Macromolecules* **2003**, *36*, 10103−10111.

(29) Junk, M. J. N.; Anac, I.; Menges, B.; Jonas, U. Analysis of optical gradient profiles during temperature- and salt-dependent swelling of thin responsive hydrogel films. *Langmuir* **2010**, *26*, 12253−12259.

(30) Raccis, R.; Roskamp, R.; Hopp, I.; Menges, B.; Koynov, K.; Jonas, U.; Knoll, W.; Butt, H.-J.; Fytas, G. Probing mobility and

structural inhomogeneities in grafted hydrogel films by fluorescence correlation spectroscopy. *Soft Matter* **2011**, *7*, 7042−7053.
(31) Ishida, N.; Biggs, S. Direct observation of the phase transition for a poly(*N*-isopropylacrylamide) layer grafted onto a solid surface by AFM and QCM-D. *Langmuir* **2007**, *23*, 11083−11088.
(32) Junk, M. J. N.; Jonas, U.; Hinderberger, D. EPR spectroscopy reveals nanoinhomogeneities in the structure and reactivity of thermoresponsive hydrogels. *Small* **2008**, *4*, 1485−1493.
(33) Bilodeau, G. G. Regular pyramid punch problem. *J. Appl. Mech.* **1992**, *59*, 519−523.
(34) Johnson, K. L. *Contact Mechanics*; Cambridge University Press: Cambridge, U.K.; 1985
(35) Harmon, M. E.; Kuckling, D.; Pareek, P.; Frank, C. W. Photo-cross-linkable PNIPAAm copolymers. 4. Effects of copolymerization and cross-linking on the volume-phase transition in constrained hydrogel layers. *Langmuir* **2003**, *19*, 10947−10956.
(36) Schild, H. G. Poly(*N*-isopropylacrylamide): experiment, theory and application. *Prog. Polym. Sci.* **1992**, *17*, 163−249.
(37) Longo, G. S.; de la Cruz, M. O.; Szleifer, I. Molecular theory of weak polyelectrolyte gels: the role of pH and salt concentration. *Macromolecules* **2011**, *44*, 147−158.
(38) Kratz, K.; Hellweg, T.; Eimer, W. Influence of charge density on the swelling of colloidal poly(*N*-isopropylacrylamide-co-acrylic acid) microgels. *Colloids Surf., A* **2000**, *170*, 137−149.
(39) Butt, H.J.-; Cappella, B.; Kappl, M. Force measurements with the atomic force microscope: technique, interpretation and applications. *Surf. Sci. Rep.* **2005**, *59*, 1−152.
(40) Butt, H. J. Measuring electrostatic, van der Waals, and hydration forces in electrolyte solutions with an atomic force microscope. *Biophys. J.* **1991**, *60*, 1438−1444.
(41) Hoare, T.; Pelton, R. Functional group distributions in carboxylic acid containing poly(*N*-isopropylacrylamide) microgels. *Langmuir* **2004**, *20*, 2123−2133.
(42) Goodman, D.; Kizhakkedathu, J. N.; Brooks, D. E. Attractive bridging interactions in dense polymer brushes in good solvent measured by atomic force microscopy. *Langmuir* **2004**, *20*, 2333−2340.
(43) Horecha, M.; Senkovskyy, V.; Synytska, A.; Stamm, M.; Chervanyov, A. I.; Kiriy, A. Ordered surface structures from PNIPAM-based loosely packed microgel particles. *Soft Matter* **2010**, *6*, 5980−5992.
(44) Annaka, M.; Morishita, K.; Okabe, S. Electrostatic self-assembly of neutral and polyelectrolyte block copolymers and oppositely charged surfactant. *J. Phys. Chem. B* **2007**, *111*, 11700−11707.
(45) Roskamp, R. F. *Functional Hydrogels*; Ph.D. Thesis,Johannes Gutenberg-Universität Mainz, 2009.
(46) Allcock, H. R. Lampe, F. W. *Contemporary Polymer Chemistry*; Prentice-Hall: Eaglewood Cliffs, NJ, 1981.
(47) Beines, P. Synthese und Charakterisierung einer Hydrogelmatrix für die Mulitanalyt-Sensorik. Ph.D. Thesis, Johannes Gutenberg-Universität Mainz, 2007.
(48) Plunkett, K. N.; Zhu, X.; Moore, J. S.; Leckband, D. E. PNIPAM chain collapse depends on the molecular weight and grafting density. *Langmuir* **2006**, *22*, 4259−4266.
(49) Pelton, R. Poly(N-isopropylacrylamide) (PNIPAM) is never hydrophobic. *J. Colloid Interface Sci.* **2010**, *348*, 673−674.
(50) Rabinovich, Y. I.; Vakarelski, I. U.; Brown, S. C.; Singh, P. K.; Moudgill, B. M. Mechanical and thermodynamic properties of surfactant aggregates at the solid-liquid interface. *J. Colloid Interface Sci.* **2004**, *270*, 29−36.